Journal of Experimental and Clinical Application of Chinese Medicine

ORIGINAL RESEARCH

Open Access

Effect of Atractylodis Macrocephalae Rhizoma-Atractylodis Rhizoma couplet medicines and its processed products on improving hyperlipidemia via promoting bile acid metabolism

Ke Li [1], Fangjie Ding [1], Liping Han [1], Jianli Gao [1,*], Zhaohuan Lou [1,*]

[1.] School of Pharmaceutical Sciences, Zhejiang Chinese Medical University, 310053 Hangzhou, Zhejiang, China

DOI: https://doi.org/10.62767/jecacm702.5499

Keywords

Hyperlipidemia

AMR-AR

FAMR-FAR

Bile acid metabolism

Lipid metabolism

Enterohepatic circulation

* **Correspondence**

Jianli Gao

School of Pharmaceutical Sciences, Zhejiang Chinese Medical University, 310053 Hangzhou, Zhejiang, China

E-mail: jianligao@zcmu.edu.cn

Zhaohuan Lou

School of Pharmaceutical Sciences, Zhejiang Chinese Medical University, 310053 Hangzhou, Zhejiang, China

E-mail: zhaohuanlou@zcmu.edu.cn

Received: 31 March 2026

Revised: 20 April 2026

Accepted: 9 May 2026

Published: 20 May 2026

Journal of Experimental and Clinical Application of Chinese Medicine 2026; 7(2): 1-21

Abstract

Background: Atractylodis Macrocephalae Rhizoma (AMR) and Atractylodis Rhizoma (AR) are medicinal-edible herbs traditionally used to regulate gastrointestinal function and metabolic homeostasis. Their products, fried AMR with bran (FAMR) and fried AR with bran (FAR) are applied to improve lipid metabolism. Increasing evidence highlights bile acid metabolism and the gut-liver axis as central regulators of lipid homeostasis. However, whether the lipid-lowering effects of AMR-AR and FAMR-FAR are mediated through bile acid remains unclear. **Objectives:** This study aimed to elucidate the characteristic effects of AMR-AR and FAMR-FAR in the treatment of hyperlipidemia and to explore their potential mechanisms of action. **Methods:** The composition changes of AMR-AR and FAMR-FAR were detected by HPLC. Hyperlipidemia was induced in mice by a high-fat diet for six weeks. Serum TC, TG, LDL-C and HDL-C levels were measured on days 11, 27, and 44. On day 44, total bile acids in serum and liver were quantified, and hepatic bile acid profiles were analyzed by UPLC-MS/MS. Hepatic histopathology and lipid accumulation were assessed by H&E and Oil Red O staining. Immunohistochemistry for hepatic lipid metabolism-related proteins and RT-qPCR for ileal cholesterol metabolism-related mRNA. Intestinal TPH1 as well as colonic FXR and TGR5 expression were evaluated by immunofluorescence. **Results:** AMR-AR significantly reduced serum TC and LDL-C levels, while both AMR-AR and FAMR-FAR markedly alleviated hepatic steatosis and inflammatory infiltration, remodeled hepatic bile acid profiles. AMR-AR enhanced hepatic LDLR, SR-BI, CYP7A1, and PPAR γ expression, whereas FAMR-FAR predominantly increased LXR α expression. AMR-AR and FAMR-FAR suppressed TPH1 and HTR4 expression in intestine, activated FXR-FGF15, upregulated bile acid transporters, and reduced colonic FXR and TGR5 expression. **Conclusions:** AMR-AR and FAMR-FAR ameliorate hyperlipidemia primarily by restoring bile acid homeostasis and coordinating gut-liver axis signaling.

1 Introduction

Along with the shift in dietary habits, obesity has emerged as a major public health concern in modern society. Accumulating evidence indicates that hyperlipidemia is significantly more prevalent in obese populations and substantially increases the risk of various cardiovascular and metabolic diseases, including atherosclerosis, hypertension, myocardial infarction, coronary heart disease, and diabetes mellitus [1]. Hyperlipidemia is generally classified into primary and secondary forms [2]. Primary hyperlipidemia is mainly caused by genetic defects combined with environmental factors and shows a clear familial predisposition [3]; whereas secondary hyperlipidemia arises from other diseases or identifiable causes [4], such as metabolic disorders, hepatic and renal diseases, thyroid dysfunction, or long-term use of certain drugs [5]. Unhealthy lifestyle factors, including poor diet, physical inactivity, and chronic stress, also play important roles in the development of hyperlipidemia [6]. Epidemiological studies have shown that the incidence and mortality of hyperlipidemia and its related complications continue to rise, accounting for nearly half of all deaths worldwide [7]. Therefore, developing safe and effective strategies for lipid intervention and prevention is of great scientific and practical significance.

Traditional Chinese medicine (TCM) has demonstrated definite efficacy and unique advantages in lipid regulation and the treatment of hyperlipidemia [8]. Compared with chemically synthesized drugs, TCM exerts lipid-lowering effects by holistically regulating lipid metabolism, with relatively mild pharmacological actions and fewer adverse effects, making it more suitable for long-term intervention and management of metabolic disorders [9]. Atractylodis Macrocephalae Rhizoma (AMR) is the dried rhizome of Atractylodes macrocephala Koidz. (Asteraceae) and is traditionally used to strengthen the spleen and stomach and to promote digestion and nutrient absorption [10]. Its major bioactive constituents include atractylenone and atractylolide. In high-fat diet (HFD)-induced obese mouse models, AMR has been shown to effectively alleviate obesity and glucose intolerance [11]. Compared with AMR, fried Atractylodis Macrocephalae Rhizoma with bran (FAMR) exhibits more pronounced effects in reinforcing spleen function and nourishing the stomach. Atractylodis Rhizoma (AR) is the dried rhizome of Atractylodes lancea (Thunb.) DC. or Atractylodes chinensis (DC.) Koidz. (Asteraceae). It is a commonly used TCM for dispelling dampness and strengthening the spleen, with recognized effects on regulating gastrointestinal function, improving dyspepsia, and eliminating internal dampness [12]. Previous studies have demonstrated that AR can significantly ameliorate body weight gain and abnormal expansion of adipose tissue [13]. Its main active components include atractylodin, atractylenone, and various volatile oils [14]. Fried Atractylodis Rhizoma with bran (FAR) also possesses spleen- and stomach-strengthening properties and is clinically used to relieve gastric distension and discomfort caused by indigestion and phlegm-dampness accumulation.

AMR and AR are frequently prescribed together as a classical spleen-tonifying herbal pair, contributing to enhanced gastrointestinal function and improved digestion and nutrient absorption. Although both are classified as medicinal herbs, according to the Catalogue of Substances Used as Both Food and Medicine, AMR and AR may also be used as food ingredients within specified dosage ranges. Molecular docking is a computational simulation approach used to predict the binding modes and affinities between small-molecule ligands and biological macromolecular receptors, such as proteins [15]. For the identified active constituents of AMR-AR and their bran-processed products (FAMR-FAR), molecular

docking analysis with relevant target proteins can provide deeper insights into their potential mechanisms of action, thereby offering a theoretical basis for improving the efficacy and safety of TCM-based interventions for hyperlipidemia [16].

Our previous studies have demonstrated that FAMR, FAR, and their processed products can effectively ameliorate hyperlipidemia [17]. However, the specific therapeutic effects and underlying mechanisms of the FAMR-FAR herbal pair remain unclear. Therefore, in the present study, a mouse model of hyperlipidemia was established by feeding mice a high-fat diet for 6 weeks. Using this model, we aimed to elucidate the characteristic effects of the AMR-AR and FAMR-FAR herbal pairs in the treatment of hyperlipidemia and to explore their potential targets from the perspectives of lipid metabolism, cholesterol metabolism, and bile acid metabolism.

2 Materials and methods

2.1 AMR-AR, FAMR-FAR water extract preparation

Raw Atractylodis Macrocephalae Rhizoma, raw Atractylodis Rhizoma, fried Atractylodis Macrocephalae Rhizoma with bran, fried Atractylodis Rhizoma with bran were provided by Zhejiang Chinese Medical University Herbal decoction pieces Co., Ltd (Hangzhou, China). Ezetimibe tablets (HJ20171017) were obtained from MSD Pharma (Singapore) Pte. Ltd (Hangzhou, China). Slices of 50g AMR-AR (1:1) or 50g FAMR-FAR (1:1) were soaked in 500mL of purified water for 30min and then subjected to reflux extraction for 1h, followed by filtration. The residues were subsequently extracted again with 400mL of purified water under reflux for 45min. The combined filtrates were concentrated under reduced pressure to a final concentration of 0.40g/mL.

High-performance liquid chromatography (HPLC) analysis was performed to quantify the major active constituents in AMR-AR and FAMR-FAR using a 2489 ultraviolet–visible detector (Waters Technology, USA). The analyzed compounds included atractylenolide I (Chengdu Pufei De, JOT-10490), atractylenolide II (Chengdu Pufei De, JOT-10489), atractylenolide III (Chengdu Pufei De, JOT-10488), atractylodin (Chengdu Must, A0547), and atractylenone (Chengdu Must, A1136). Chromatographic separation was achieved using an XB-C18 column (4.6 × 250 mm, 5 μm; Welch Materials, Inc.). The detection wavelength was set at 243 nm, the column temperature was maintained at 30°C, the flow rate was 1.0 mL/min, and the injection volume was 10 μL. The mobile phase consisted of solvent A (acetonitrile) and solvent B (ultrapure water), with gradient elution as follows: 0-10 min, 48%-50% A; 10-20 min, 50%-70% A; and 20-40 min, 70%-80% A.

2.2 Animals grouping and treatments

Thirty SPF-grade male C57BL/6 mice (18-21 g) were obtained from Slack (China; license number: SCXK (Shanghai) 2017-0005). The mice were housed at the Animal Experimental Center of Zhejiang Chinese Medical University (IACUC No. 20210726-07) under controlled environmental conditions, with a temperature of 20-25 ° C, relative humidity of 50%-60%, and a 12 h light/dark cycle.

After one week of adaptation, 30 mice were randomly assigned into 5 groups: normal control (NC) group, model control (MC) group, Ezetimibe positive control (Ezetimibe) group, AMR-AR group, and FAMR-FAR groups, 6 mice per group. Except for the NC group, all mice were fed a high-fat diet (HFD, D12109C, Changzhou Shuyi Shuer, China) for 6 weeks. The HFD mainly consisted of 23.51% corn starch, 22.18% casein, 17.19% cocoa butter, 12.53% sucrose, 1.25% cholesterol, and 0.50% sodium cholate and so on. The experiment was conducted with simultaneous modeling and drug administration, mice in the NC and MC groups were administered an equal volume of purified water by gavage. The ezetimibe group

received ezetimibe suspension at a dose of 1.52 mg/kg by gavage, while the AMR-AR and FAMR-FAR groups were administered AMR-AR and FAMR-FAR aqueous extracts, respectively, at a dose of 4.0 g/kg by gavage. After six weeks of continuous intervention with once-daily oral gavage administration, mice were euthanized by exposure to high concentrations of carbon dioxide following the final dose. Liver, small intestine, and colon tissue samples were collected immediately thereafter and preserved by freezing for subsequent experimental use.

2.3 Biochemical assay

On days 11, 27, and 44 following the administration intervention, blood samples were collected from mice under deep isoflurane anesthesia. A capillary blood collection tube was then inserted from the inner canthus with a rotating motion to a depth of approximately 2-5 mm. After blood flow was observed, the tube was withdrawn, and light pressure was applied to achieve hemostasis. A blood volume of 0.2-0.3 mL was collected per mouse per time point. The collected blood was allowed to stand at room temperature for 30 min, and then centrifuged at 3500 rpm for 10 min at 4°C to separate the serum. TC (Nanjing Jiancheng, A111-1-1, China), TG (Nanjing Jiancheng, A110-1-1, China), HDL-C (Nanjing Jiancheng, A112-1-1, China), LDL-C (Nanjing Jiancheng, A113-1-1, China), and TBA (Nanjing Jiancheng, E003-2-1, China) levels were measured using corresponding commercial assay kits with a Power Wave 340 microplate reader (BioTek Instruments, Inc., Winooski, VT, United States).

2.4 Bile acids analysis

The bile acid composition in mouse liver tissues was analyzed using an Agilent 1290 ultra-performance liquid chromatography system coupled with a 6495 triple quadrupole mass spectrometer (UPLC-MS/MS). This analytical method was optimized and recommended by LC-Biotechnology Co., Ltd. (Hangzhou) based on existing established protocols.

2.5 Hematoxylin and Eosin (H&E), Oil-red-O staining of liver tissue

Liver tissue specimens were dehydrated and embedded in paraffin, then sectioned into 4 μm slices. Following conventional dewaxing and hydration, sections were sequentially stained with hematoxylin for 5 min and with eosin for 3 min 30 s. Histopathological changes were observed and photographed under a microscope. Hepatic lipid accumulation was assessed using Oil Red O staining: liver tissues were embedded in OTC compound and rapidly frozen, fixed in 10% formalin for 10 min, and then rinsed. The sections were briefly immersed in 60% isopropanol for 30 s to remove excess moisture. The slices were incubated in modified Oil Red O solution for 10 min and subsequently rinsed with 60% isopropanol to remove residual dye. Cell nuclei were counterstained with Mayer's hematoxylin for 1 min and rinsed with water.

2.6 Alcian blue-periodic acid schiff (AB-PAS) staining

AB-PAS staining was used to examine glycogen changes in the colonic tissues of hyperlipidemic mice. The procedure was as follows: paraffin-embedded colonic tissue sections were first deparaffinized and hydrated; the sections were then sequentially stained with Schiff's reagent, periodic acid solution, and Alcian blue dye. Finally, the slides were cleared with xylene and mounted with neutral resin for observation.

2.7 Immunohistochemistry (IHC)

To detect lipid metabolism in liver tissue, paraffin sections of liver tissues were taken for routine IHC to observe the expression of PCSK9 (Proteintech, 55206-1-AP, China), LDLR (Proteintech, 10785-1-AP, China), SR-BI (NOVUS, NB400-104, China), CYP7A1 (Affinity, DF2612, China), PPARγ (Affinity, AF6284, China), LXRα (NOVUS, NBP2-66938, China), ABCG1 (Proteintech, 13578-1-AP, China) in the liver tissue.

Tissue images were captured using a biological optical microscope, and immunohistochemical staining was semi-quantitatively analyzed using ImageJ software (National Institutes of Health, USA).

2.8 Immunofluorescent staining (IF)

To detect bile acid metabolism, paraffin sections of colonic and small intestine tissue were dewaxed and hydrated conventionally and then underwent antigen restoration. 3% hydrogen peroxide was used to eliminate endogenous catalase activity, and QuickBlock Immunol Staining Blocking Buffer dilution (Beyotime, P0260, China) was blocked. Incubate with antibody of TPH1 (Affinity, DF6465, China), TGR5 (ABCAM, ab72608, UK), FXR (Cell Signaling, 12295S, United States) at 4℃ overnight. TPH1 incubated with FITC-labeled Goat Anti-Rabbit IgG (H+L) (Beyotime, A0562, China), then the slices were stained with DAPI and subsequently sealed. Co-staining of TGR5, FXR, and DAPI was performed using a Four-color Fluorescence kit (Recordbio, China) based on the tyramide signal amplification (TSA) technology according to the instruction.

2.9 Real-time quantitative PCR (RT-qPCR)

Total RNA was extracted from ileal tissues using a SteadyPure RNA Extraction kit (Accurate, AG21024, China). The Evo M-MLV reverse transcription premix kit (Accurate, AG11728, China) was used to synthesize cDNA. RT-qPCR amplification was performed in StepOne™RealTime PCR using the SYBR Green Pro Taq HS Premixed qPCR kit (High ROX) (AG11740, Accurate Biotechnology, Hunan, China). Predenaturation: 95°C for 30 s; denaturation: 95°C for 5 s; annealing extension: 60°C for 30 s, 40 cycles. Gene mRNA expression was calculated using the 2-ΔΔ CT method. Primers of the genes, including GAPDH, TPH1, HTR4, FXR, FGF15, ASBT, OSTα, ABCG5, and ABCG8, were synthesized by Sangon Bioengineering (Shanghai) Co., LTD (Shanghai, China) (Table 1).

Table 1 Oligonucleotide primers used for real-time PCR analysis.

Gene	Forward(5'to3')	Reverse (5'to3')
ABCG5	CGCAGGGACCGAATTGTGATTG	ACACCAACTCTCCGTAAGTCAGG
ABCG8	GCAACTTCACCTTCTCCATCCTC	CTGATGCCGATGACAATGAGGTAG
ASBT	CCACTTGCTCCACACTGCTTG	TCCCGAGTCAACCCACATCTTG
FGF15	CCTGTACTCCGCTGGTCCCTATG	GGTCCTCCTCGCAGTCCACAG
FXR	ACAGAGAGGCGGTGGAGAAGC	TCAGCGTGGTGATGGTTGAATGTC
GAPDH	AGAAGGTGGTGAAGCAGGCATC	CGAAGGTGGAAGAGTGGGAGTTG
HTR4	GGCTGGAACAACATCGGCATAG	ACAGAGCAGGTGATAGCATAGGG
OSTα	CACATGCTCATACTGGAGACCTTC	GCAGCGAACAAGCCTCATACC
TPH1	CGACATCAGCCGAGAACAGTTG	CATAACGTCTTCCTTCGCAGTGAG

2.10 Protein-ligand molecular docking

Proteins closely associated with lipid metabolism, lipid transport, and bile acid metabolism observed in the experiments were selected as molecular docking targets, including PCSK9 (PDB ID: 2P4E), LDLR (PDB ID: 3OFF), CYP7A1 (PDB ID: 3V8D), PPARγ (PDB ID: 2Q59), LXRα (PDB ID: 3IPQ), ABCG1 (PDB ID: 7R8D), TGR5 (PDB ID: 7CFM), FXR (PDB ID: 1OSH), and TPH1 (PDB ID: 5TPG). The three-dimensional structures of these target proteins were obtained from the Protein Data Bank (PDB; https://www.rcsb.org/).

The molecular structures of the active constituents were downloaded from the PubChem database in SDF format and subjected to molecular docking analysis using the CB-Dock2 platform (https://cadd.labshare.cn/cb-dock2/index.php). Prior to docking, the protein receptors were preprocessed by removing water molecules and adding hydrogen atoms. Each small-molecule ligand was then docked individually with the corresponding target protein to calculate binding energies, and the docking results were subsequently visualized.

2.11 Statistical analysis

GraphPad Prism 9.0 software (San Diego, California, USA) was used for drawing diagrams. All quantitative results were expressed as mean ± standard deviations (SD), and statistical differences between the groups were evaluated through a two-tailed Student ' s t-test or one-way analysis of variance (ANOVA). $P<0.05$ was considered to have a statistically significant difference.

3 Results

3.1 Content determination of components both in AMR-AR and FAMR-FAR

High-performance liquid chromatography (HPLC) was employed to determine the major active constituents in AMR-AR and FAMR-FAR. By comparison with corresponding reference standards, a semi-quantitative analysis was performed to evaluate the changes in atractylenolide III, atractylenolide II, atractylenolide I, atractylodin, and atractylone in AMR-AR and FAMR-FAR (Figure 1, Table 2). The results showed that the contents of all these components were increased in FAMR-FAR compared with AMR-AR, indicating that processing may promote the transformation and enrichment of these constituents.

3.2 AMR-AR and FAMR-FAR improved symptoms in hyperlipidemia mice

A hyperlipidemic mouse model was established by feeding mice a HFD for six weeks. The results demonstrated that a HFD not only altered hair metabolic status but also markedly affected hair growth. During model induction, mice in the MC group exhibited progressive whisker loss, and in severe cases, hair depigmentation was observed on the cheeks and back. Treatment with AMR-AR and FAMR-FAR significantly alleviated whisker loss in mice (Figure 2A). Body weight analysis showed a fluctuating upward trend in the MC group, whereas administration of AMR-AR and FAMR-FAR slightly attenuated weight gain (Figure 2B). Meanwhile, the liver index was significantly increased in the MC group compared with the NC group (Figure 2C, $P<0.001$), and both AMR-AR and FAMR-FAR treatments markedly reduced the liver index.

The results of the four items of blood lipids in the serum that a HFD profoundly disrupted lipid metabolic homeostasis in mice. Relative to the NC group, mice in the MC group exhibited persistently elevated serum TC levels on days 11, 27, and 44 (Figure 2D, $P<0.001$). Following AMR-AR and FAMR-FAR administration, TC levels showed an overall downward trend, with a pronounced reduction observed in the AMR-AR group on day 44 versus the MC group ($P<0.001$). Given the dynamic nature of lipid metabolism, serum TG levels

displayed time-dependent variations. On day 27, TG levels in the MC group were lower than those in the NC group, yet remained markedly higher than those in all treatment groups; intervention with AMR-AR and FAMR-FAR substantially attenuated TG levels (Figure 2E, P<0.01). By day 44, TG levels in the MC group were again elevated compared with the NC group (P<0.05), whereas treatment resulted in an evident downward tendency. Meanwhile, LDL-C levels were consistently increased in the MC group at days 11, 27, and 44 (Figure 2F, P<0.001). Both AMR-AR and FAMR-FAR effectively counteracted these abnormalities. Notably, a significant reduction in LDL-C was observed in the FAMR-FAR group as early as day 11 (P<0.05), whereas a delayed but distinct decrease was detected in the AMR-AR group on day 44 (P<0.05). HDL-C levels were markedly reduced in the MC group throughout the experimental period (Figure 2G). Versus the MC group, administration of AMR-AR or FAMR-FAR resulted in varying degrees of improvement in HDL-C levels. These results indicate that AMR-AR and FAMR-FAR intervention may partially restores lipid metabolic balance and alleviates the hyperlipidemic phenotype in mice.

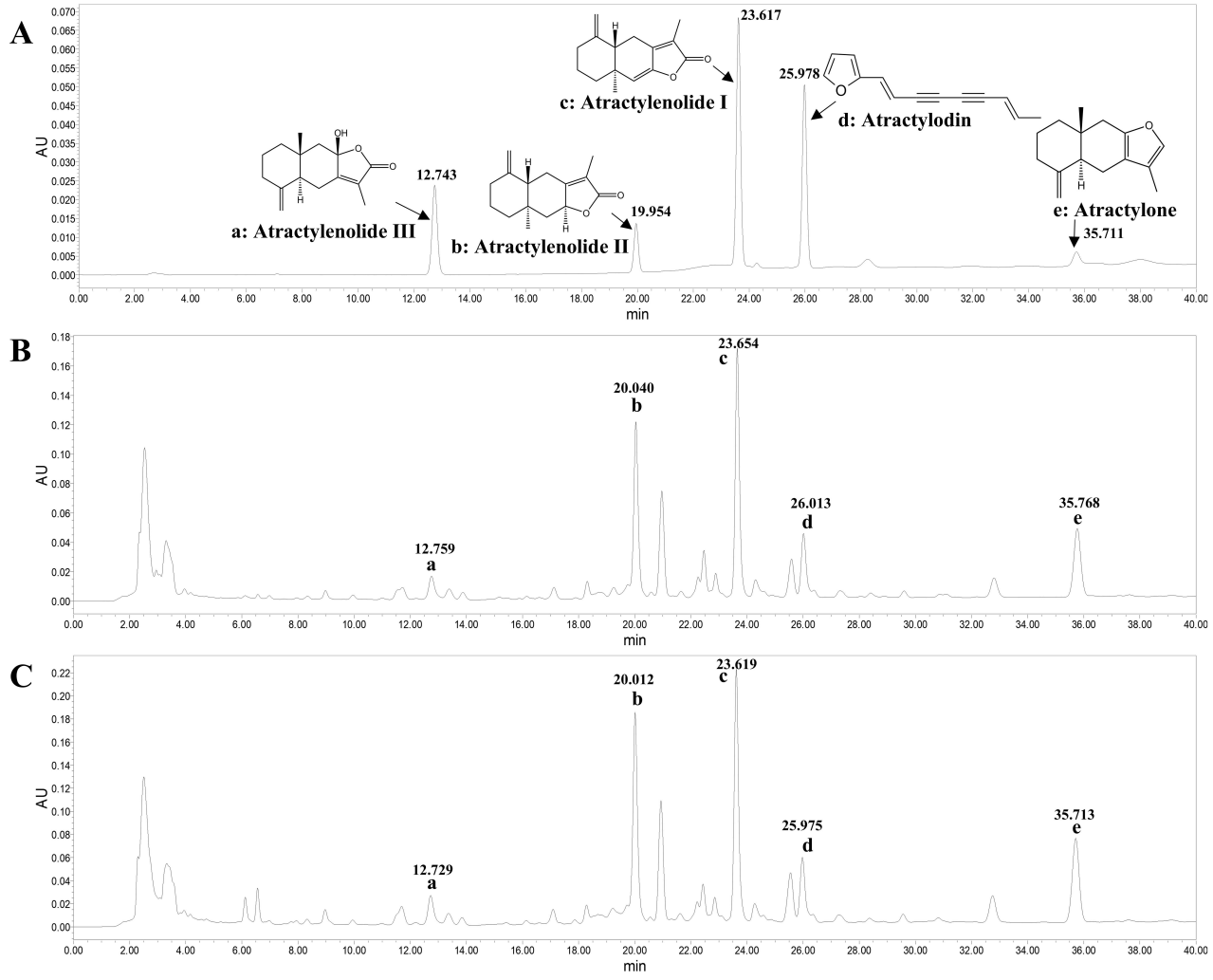

Figure 1 HPLC spectra of standard and AMR-AR and FAMR-FAR samples. (A) Spectra of standard samples (a. Atractylenolide III, retention time: 12.743 min; b. Atractylenolide II, retention time (Rt): 19.945 min; c. Atractylenolide I, Rt: 23.617 min; d. Atractylodin, Rt: 25.978 min; e. Atractyone, Rt: 35.711 min). (B) HPLC spectra of AMR-AR. (C) HPLC spectra of FAMR-FAR.

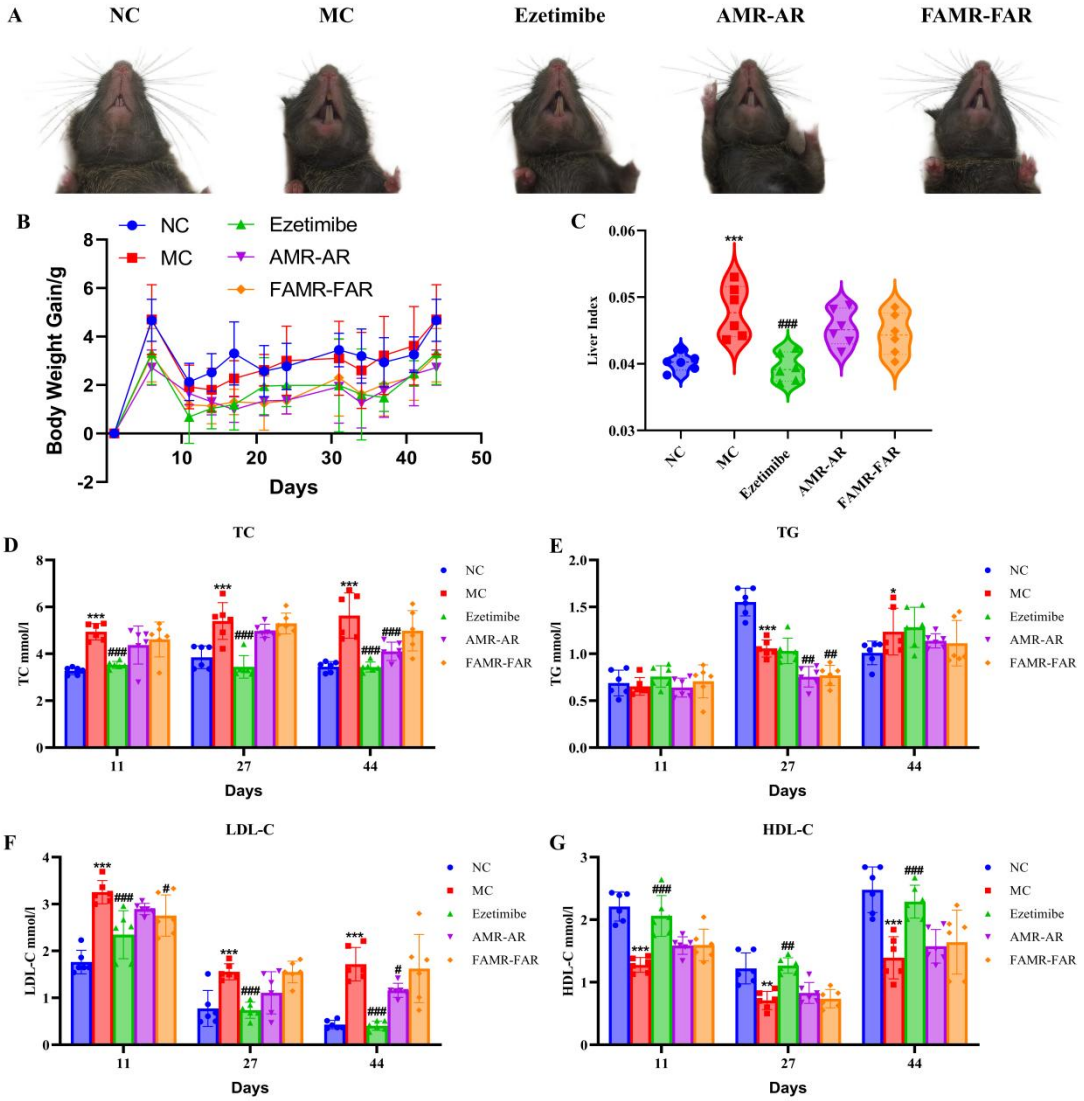

Figure 2 AMR-AR and FAMR-FAR improved symptoms in hyperlipidemia mice. (A) Whisker changes in different groups of mice. (B) Changes in body weight (n=6). (C) Liver coefficients of mice (n=6). (D) TC levels in the serum (n=6). (E) TG levels in the serum (n=6). (F) LDL-C levels in the serum (n=6). (G) HDL-C levels in the serum (n=6). Compared with NC group, *p< 0.05, **p< 0.01 and ***p< 0.001; compared with MC group, #p< 0.05, ##p< 0.01 and ###p< 0.001.

Table 2 The contents of components in AMR-AR and FAMR-FAR.

Sample	Components content (mg/g)				
	Atractylenolide III	Atractylenolide II	Atractylenolide I	Atractylodin	Atractylone
AMR-AR	0.61	3.43	2.11	0.31	5.12
FAMR-FAR	0.93	5.40	2.84	0.42	8.09

3.3 AMR-AR and FAMR-FAR improve the histopathological changes in hyperlipidemic mice

Gross morphological examination showed that livers from mice in the NC group were bright red in color, with a regular shape and normal size, whereas livers from the MC group exhibited a pale orange appearance. Compared with the MC group, treatment with AMR-AR and FAMR-FAR markedly improved the gross liver appearance (Figure 3A). To further evaluate the effects of AMR-AR and FAMR-FAR on HFD-induced hepatic steatosis, histopathological analyses were performed. H&E staining revealed that hepatocytes in the NC group were radially and orderly arranged around the central vein. In contrast, liver sections from the MC group displayed extensive hepatocellular vacuolar degeneration accompanied by pronounced inflammatory cell infiltration (Figure 3B, yellow arrows). Following AMR-AR and FAMR-FAR intervention, lipid vacuolization was markedly reduced, hepatocellular architecture was largely restored, and inflammatory infiltration was substantially alleviated. Consistently, Oil Red O staining demonstrated abundant brown-red lipid droplet accumulation in the livers of MC mice, whereas treatment with AMR-AR and FAMR-FAR significantly decreased intracellular lipid deposition (Figure 3C, white circles).

In addition, H&E and AB-PAS staining of colonic tissues showed a pronounced thickening of the submucosal layer accompanied by reduced mucin secretion in the MC group (Figure 3D-E, green arrows). Following AMR-AR and FAMR-FAR treatment, the distribution and expression of mucins in the colonic mucosa were markedly restored (Figure 3E, black arrows). Collectively, these findings indicate that AMR-AR and FAMR-FAR intervention effectively ameliorates HFD-induced hyperlipidemia-associated hepatic steatosis and significantly corrects abnormalities in colonic mucin secretion.

3.4 Molecular docking of major active components in AMR-AR and FAMR-FAR with core proteins involved in lipid metabolism

Differences in therapeutic efficacy among formulations are generally attributable to variations in the composition and abundance of their bioactive constituents. To further elucidate the potential interactions between the major active components of AMR-AR and FAMR-FAR (Atractylenolide I, Atractylenolide II, Atractylenolide III, Atractylodin, and Atractylone) and key proteins involved in lipid and bile acid metabolism, a systematic molecular docking analysis was performed. Docking outcomes were evaluated based on binding energy values, with red and blue indicating relatively higher and lower binding energies, corresponding to weaker and stronger binding affinities, respectively. In general, binding energies below -7 kcal/mol are considered indicative of favorable interactions, while -9 kcal/mol serves as a reference threshold for potential drug-like activity, with complexes below this value regarded as promising candidates for further development. As shown in Figures 4A-B, multiple active components exhibited low binding energies with LXRα, FXR, TGR5, and ABCG1, suggesting a capacity to engage key regulatory targets associated with lipid and bile acid metabolism. These findings imply that the active constituents of AMR-AR and FAMR-FAR may exert anti-hyperlipidemic effects through coordinated interactions with multiple metabolic targets. Furthermore, representative ligand-protein complexes with the lowest binding energies and high conformational stability were selected from each group and visualized in three-dimensional models to illustrate their interaction patterns (Figures 4C-K).

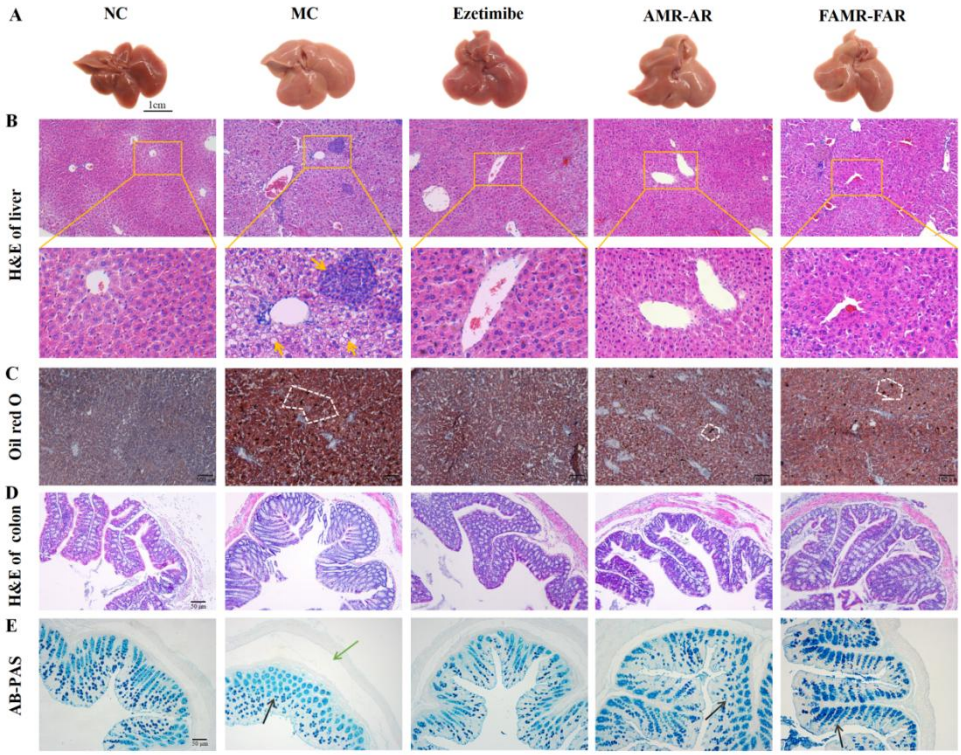

Figure 3 AMR-AR and FAMR-FAR improve the histopathological changes in hyperlipidemic mice. (A) General view of the liver in each group. (B) Liver histopathology (H&E staining, 100×, 200×). (C) Oil red O staining of liver tissues. (D) Colon histopathology (H&E staining, 100×). (E) AB-PAS staining of colon (200×).

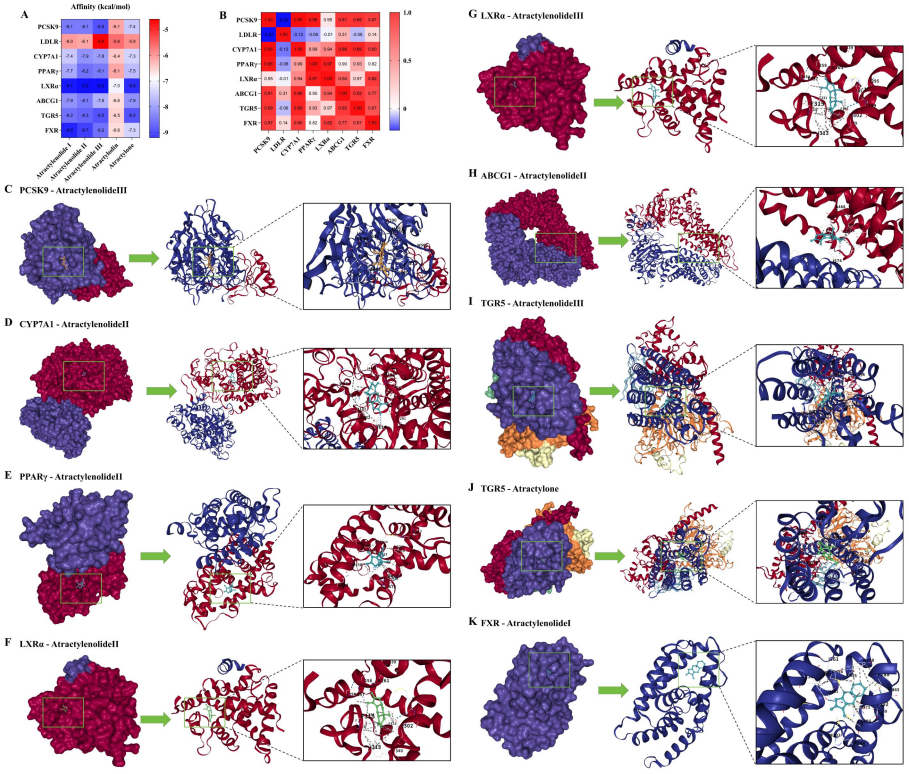

Figure 4 AMR-AR and FAMR-FAR Molecular docking results. (A) Molecular docking results between active components and core proteins of AMR-AR and FAMR-FAR. (B) Correlation analysis of molecular docking results. (C-K) Representative molecular docking results were visualized.

3.5 AMR-AR and FAMR-FAR promoted liver cholesterol metabolism in mice with hyperlipidemea

Based on the molecular docking predictions, IHC staining was subsequently performed on liver tissues to evaluate the effects of AMR-AR and FAMR-FAR on lipid metabolism-related pathways. PCSK9 is a key regulator of circulating LDL-C levels by modulating the stability and degradation of LDLR, whereas LDLR maintains cholesterol homeostasis through the clearance of LDL-C from the bloodstream. SR-BI facilitates cholesterol transport and metabolism, particularly mediating hepatic uptake of HDL-C [18]. In addition, CYP7A1 catalyzes the rate-limiting step in bile acid synthesis from cholesterol and is therefore critical for cholesterol catabolism and excretion.

IHC analysis revealed that, compared with the NC group, the MC group exhibited a marked upregulation of PCSK9 expression (Figure 5A), accompanied by reduced expression of LDLR and CYP7A1 and a pronounced decrease in SR-BI expression (Figure 5B-D, $P<0.05$). Following drug intervention, PCSK9 expression was decreased in both the AMR-AR and FAMR-FAR groups relative to the MC group. Notably, AMR-AR treatment significantly increased the expression of LDLR and SR-BI ($P<0.01$, $P<0.05$), with a modest elevation in CYP7A1 expression, whereas FAMR-FAR treatment also reversed these pathological alterations to varying extents. These findings indicate that both AMR-AR and FAMR-FAR enhance hepatic cholesterol metabolism, with AMR-AR exerting a more pronounced regulatory effect.

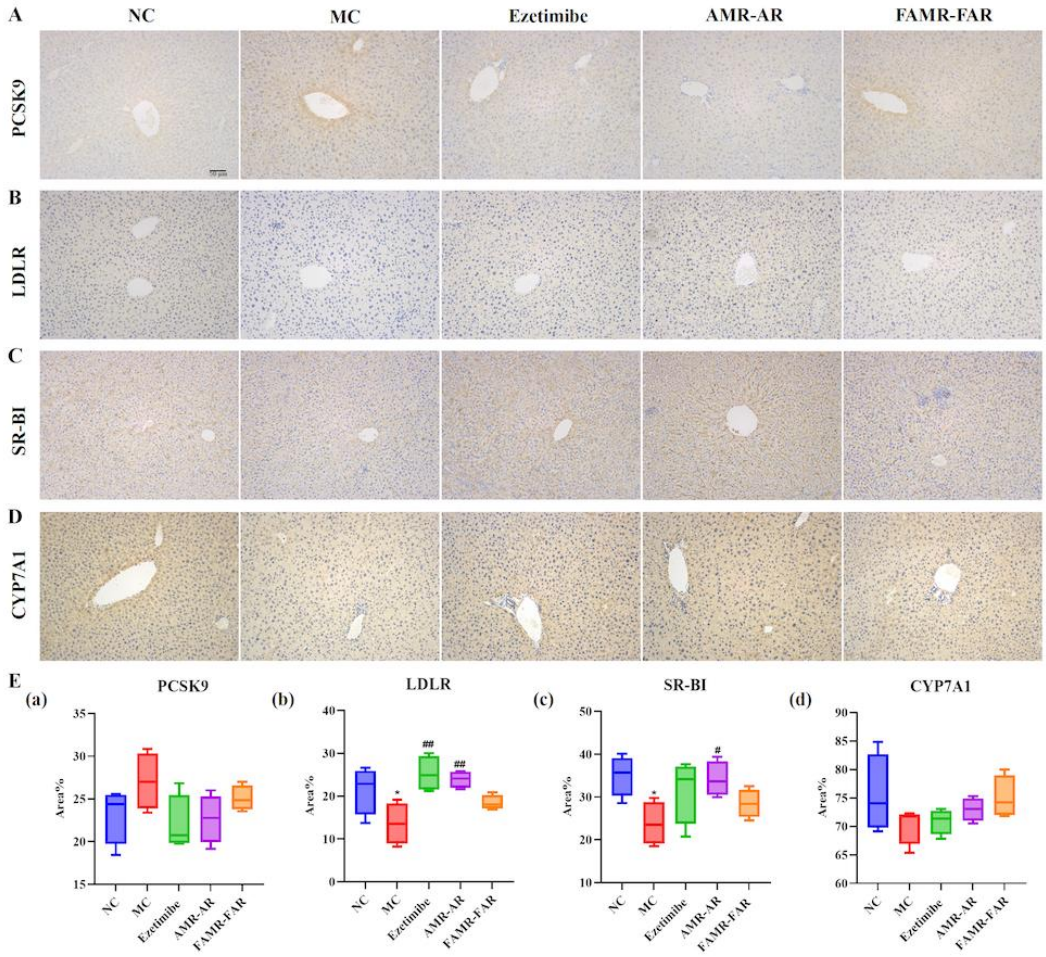

Figure 5 AMR-AR and FAMR-FAR influence liver cholesterol metabolism in hyperlipidemic mice. (A-D) Expression of PCSK9, LDLR, SR-BI and CYP7A1 in liver tissues (200×). (E) Immunohistochemistry quantitative analyses (n=3). Compared with NC group, *p< 0.05; compared with MC group, #p< 0.05, ##p< 0.01.

Cholesterol reverse transport represents a critical pathway in cholesterol metabolism. The PPARγ-LXRα -ABCG1 signaling axis positively regulates lipid homeostasis in the circulation by promoting ABCG1-mediated cholesterol efflux [19]. IHC analysis demonstrated that the expression levels of PPARγ, LXRα, and ABCG1 were significantly reduced in the MC group compared with the NC group (Figure 6A-D, P<0.05). Treatment with AMR-AR or FAMR-FAR effectively reversed these decreases. Notably, AMR-AR treatment resulted in a significant upregulation of ABCG1 expression (P<0.05), whereas FAMR-FAR treatment markedly increased LXR α expression (P<0.05). These findings indicate that both AMR-AR and FAMR-FAR facilitate cholesterol reverse transport through modulation of the PPAR γ -LXR α -ABCG1 pathway, albeit with distinct regulatory preferences.

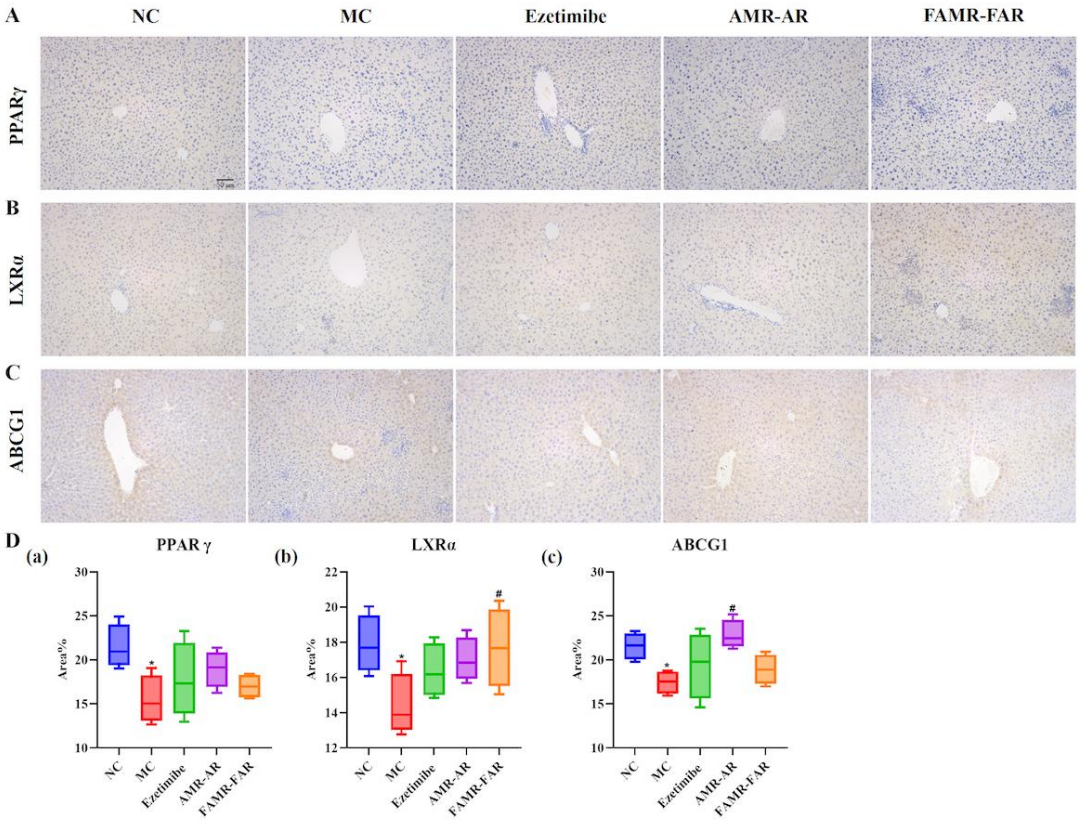

Figure 6 AMR-AR and FAMR-FAR promote the process of reverse cholesterol transport. (A-C) Expression of PPAR γ, LXRα, and ABCG1 in liver tissues 200×). (D) Immunohistochemistry quantitative analyses (n=3). Compared with NC group, *p< 0.05; compared with MC group, #p< 0.05.

3.6 AMR-AR and FAMR-FAR affect bile acid metabolism in mice with hyperlipidemea induced by the HFD

To further substantiate the regulatory effects of AMR-AR and FAMR-FAR on bile acid metabolism, total bile acid (TBA) levels in serum and liver tissues were quantified, and the hepatic bile acid composition was profiled by UPLC-MS/MS. The results showed that TBA levels in both serum and liver were significantly elevated in the MC group compared with the NC group (Figure 7A-B, P<0.05). Following AMR-AR or FAMR-FAR treatment, serum TBA levels were markedly reduced, whereas hepatic TBA levels were further increased, suggesting enhanced hepatic bile acid sequestration and altered bile acid distribution.

Principal component analysis (PCA) revealed a clear separation between the NC and MC groups, indicating profound alterations in bile acid profiles induced by

high-fat feeding. In contrast, the AMR-AR and FAMR-FAR groups partially overlapped with the NC group, with overlap between the two treatment groups, reflecting a convergence toward a normalized bile acid metabolic pattern (Figure 7C). Pearson correlation analysis of hepatic bile acid species demonstrated strong inter-component correlations across groups (Figure 7D). Consistently, heatmap visualization of hepatic bile acid composition showed pronounced differences between the NC and MC groups, whereas both AMR-AR and FAMR-FAR induced marked shifts relative to the MC group, highlighting their robust impact on bile acid metabolism (Figure 7E).

Quantitative analysis of individual bile acid species identified from the heatmap further revealed that, compared with the NC group, the MC group exhibited a significant reduction in multiple FXR-antagonistic and TGR5-agonistic bile acids, including α/ω-MCA, HCA, ACA, UCA, HDCA, THDCA and MDCA ($P<0.05$, $P<0.001$), accompanied by a pronounced increase in the potent FXR agonist GCDCA (Figure 7F, $P<0.001$). This bile acid signature indicates severe disruption of bile acid homeostasis under high-fat diet conditions, characterized by excessive FXR activation, impaired bile acid synthesis, suppression of cholesterol catabolism, attenuation of TGR5-mediated metabolic signaling, and compromised gut microbiota-dependent bile acid transformation, collectively contributing to persistent dyslipidemia.

Compared with the MC group, both AMR-AR and FAMR-FAR interventions significantly reduced hepatic GCDCA levels ($P<0.001$, $P<0.01$), effectively alleviating excessive FXR-driven negative feedback. Notably, AMR-AR preferentially increased the FXR-antagonistic bile acid T-β-MCA ($P<0.05$), as well as the TGR5-agonistic bile acids DCA and TLCA ($P<0.05$), suggesting coordinated modulation of FXR and TGR5 signaling to enhance cholesterol catabolism and energy metabolism. In contrast, FAMR-FAR predominantly elevated GCA levels ($P<0.05$), reflecting restoration of bile acid synthesis and bile acid pool composition, thereby promoting cholesterol elimination in a more homeostatic and stabilized manner.

3.7 AMR-AR and FAMR-FAR affect bile acid metabolism in mice with hyperlipidemea induced by the HFD

Previous studies have demonstrated that pharmacological inhibition of HTR4 markedly ameliorates HFD-induced fatty liver in mice [20]. Consistent with this notion, immunofluorescence staining of small intestinal tissues revealed a pronounced increase in TPH1 expression in the MC group, which was effectively reversed by AMR-AR and FAMR-FAR treatment (Figure 8A). RT-qPCR analysis further confirmed that ileal Tph1 mRNA levels were significantly elevated in the MC group compared with the NC group, whereas both AMR-AR and FAMR-FAR markedly suppressed this increase (Figure 8B). In parallel, HTR4 expression was significantly upregulated in the MC group (Figure 8C, $P<0.05$), indicating aberrant activation of intestinal serotonergic signaling. This elevation was effectively attenuated following AMR-AR or FAMR-FAR intervention ($P<0.05$).

Moreover, the mRNA expression of key bile acid reabsorption–related factors, including FXR, FGF15, ASBT, and OSTα, was markedly reduced in the ileum of MC mice (Figure 8D-G), reflecting impaired bile acid sensing and enterohepatic feedback. Notably, AMR-AR and FAMR-FAR treatment reversed these abnormalities, with a particularly robust induction of FGF15 expression ($P<0.01$). Given that FXR activation also induces the expression of the cholesterol efflux transporters ABCG5 and ABCG8, their transcriptional levels were further examined. Compared with the NC group, MC mice exhibited a modest compensatory

increase in ABCG5 and ABCG8 mRNA expression, whereas AMR-AR and FAMR-FAR intervention further enhanced their expression, suggesting facilitation of cholesterol excretion.

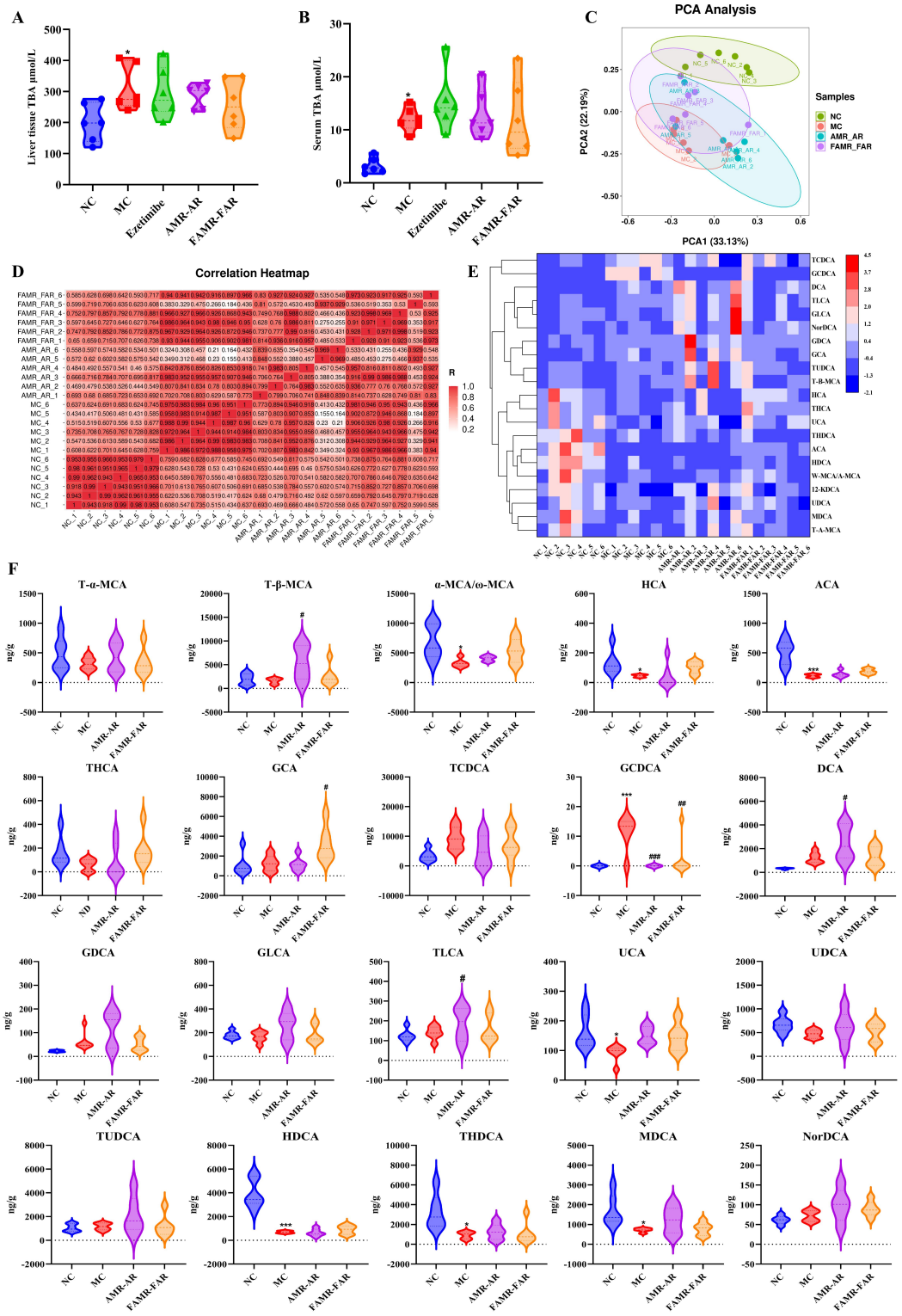

Figure 7 AMR-AR and FAMR-FAR affect bile acid metabolism. (A) TBA levels in Serum (n=6). (B) TBA levels in liver tissue (n=6). (C) PCA of liver tissue BA profiles (n=6). (D) Pearson correlation coefficient of liver tissue BA profile. (E) Heat map of BA profiles in liver tissue (n=6). (F) Changes in the content of representative BAs in liver tissue (n=6). Compared with NC group, *p< 0.05 and ***p< 0.001; compared with MC group, #p< 0.05, ##p< 0.01 and ###p< 0.001.

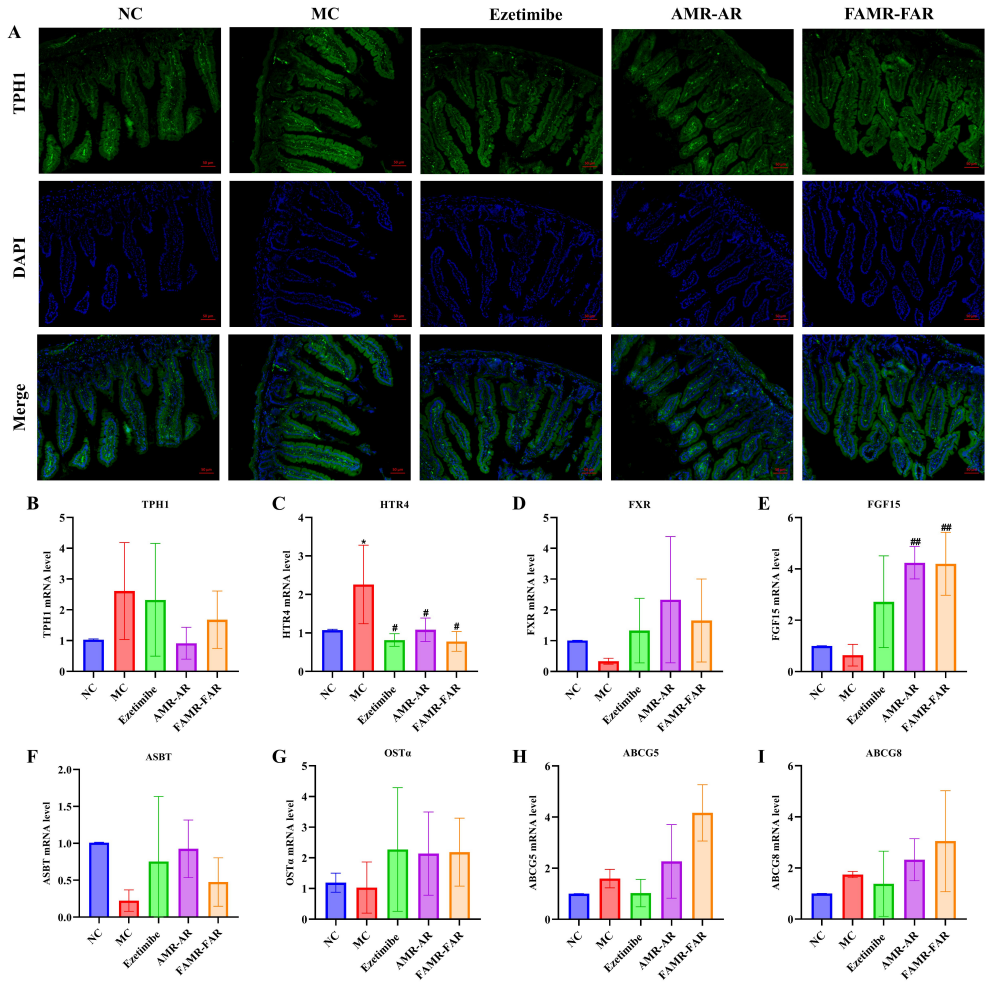

Figure 8 AMR-AR and FAMR-FAR regulate the expression of genes involved in bile acid metabolism in the small intestine (A) Immunofluorescence staining of the small intestine (200×). (B-I) Relative mRNA expression of bile acid metabolism-related genes in ileum tissue of mice in each group (n=3). Compared with NC group, *p< 0.05 and ***p< 0.001; compared with MC group, #p< 0.05, ##p< 0.01 and ###p< 0.001.

Collectively, these findings indicate that HFD disrupts intestinal bile acid sensing and enterohepatic feedback while concomitantly inducing aberrant activation of the Tph1/5-HT/HTR4 axis. AMR-AR and FAMR-FAR effectively suppress excessive serotonergic signaling and restore FXR/FGF15 mediated bile acid reabsorption and feedback regulation, thereby promoting cholesterol elimination and re-establishing bile acid metabolic homeostasis.

3.8 AMR-AR and FAMR-FAR regulate bile acid metabolic disorders in mice with hyperlipidemea induced by HFD

Previous studies have reported that a HFD could markedly increases fecal bile acid excretion [21]. Consistent with this alteration in bile acid handling, multiplex immunofluorescence analysis revealed that FXR and TGR5 were predominantly localized in colonic epithelial cells (Figure 9A-B), compared with the NC group, the MC group exhibited significantly enhanced fluorescence intensities of both FXR and TGR5 (P<0.05), indicating aberrant activation of bile acid-responsive signaling in the colon. Notably, AMR-AR and FAMR-FAR treatment effectively reversed these changes. Specifically, FAMR-FAR significantly attenuated FXR expression (P<0.05), whereas

AMR-AR predominantly reduced TGR5 expression (P<0.05), suggesting distinct yet complementary regulatory effects on colonic bile acid signaling.

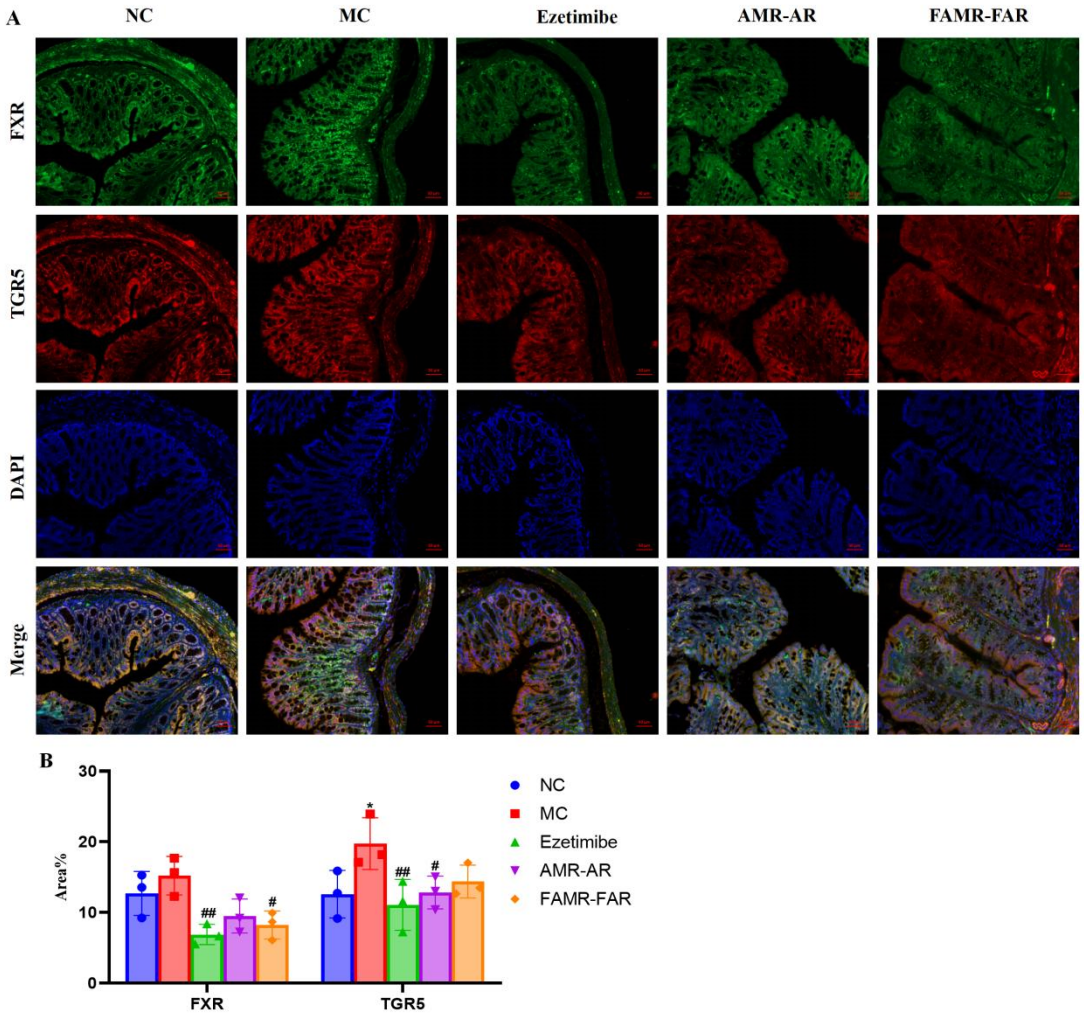

Figure 9 AMR-AR and FAMR-FAR regulate metabolic disorders in hyperlipidemic mice. (A) Multiple immunofluorescence staining for FXR and TGR5 in colon (200×). (B) FXR and TGR5 quantitative analyses (n=3). Compared with NC group, *p< 0.05; compared with MC group, #p< 0.05, ##p< 0.01 and ###p< 0.001.

4 Discussion

Among traditional processing methods, stir-frying with wheat bran is the most widely used and representative technique for both Atractylodes species [22], exerting a well-defined directional modulation of their medicinal properties. Previous studies have shown that stir-frying with wheat bran alters the composition of volatile oils and improves the bioavailability of lipophilic constituents, gastrointestinal irritation while enhancing affinity toward the middle-jiao digestive and metabolic system. Therefore, based on traditional Chinese medicine theory and modern pharmacology, AMR-AR and FAMR-FAR are also applicable to chronic metabolic disorders characterized by lipid metabolism dysregulation.

The therapeutic effects of Chinese herbal medicine originate from their inherent chemical constituents, and the processing of herbs influences their medicinal properties by altering their material basis and biological activities. The principal active components of AMR are atractylenolides I, II, and III, whereas AR primarily derives its pharmacological activity from volatile oil and polyacetylene compounds, including

atractylodin and atractylone. In our study, HPLC was employed to quantify and compare the major active constituents in AMR-AR and FAMR-FAR. The results showed that stir-frying with wheat bran increased the contents of key components in both herbal slices to varying degrees, suggesting a close relationship between compositional changes and the processing method. On this basis, molecular docking was further performed to evaluate the interactions between these components and key targets involved in lipid and bile acid metabolism, thereby predicting their potential therapeutic effects.

Although hyperlipidemia is often accompanied by obesity, no significant changes in body weight were observed in either the HFD model group or the treatment groups in this study. However, histopathological examination revealed that all animals after modeling developed typical hepatic steatosis, characterized by elevated serum levels of TC, TG, and LDL-C, as well as decreased HDL-C. Pathological staining further demonstrated obvious lipid accumulation in liver tissues. These findings suggest the occurrence of visceral obesity—a condition in which fat is abnormally deposited in internal organs such as the liver without substantial alterations in body weight. Compared with generalized obesity, visceral obesity is more insidious and easily overlooked by routine body weight monitoring. Nevertheless, it is closely associated with an increased risk of metabolic syndrome, insulin resistance, and cardiovascular diseases. Therefore, when evaluating the efficacy of interventions for hyperlipidemia, one should not rely solely on body weight as an indicator. Instead, a comprehensive assessment integrating histopathological and metabolic parameters is essential to fully elucidate the true therapeutic effects and potential risks of the interventions.

Reverse cholesterol transport (RCT) depends on HDL to transport excess cholesterol from peripheral tissues to the liver [23]. Hepatic clearance of LDL-C is primarily mediated by LDLR, a process negatively regulated by PCSK9: elevated PCSK9 promotes LDLR degradation, reduces LDL-C uptake, and leads to increased circulating LDL-C levels [24]. In addition, ABCG1 is a key cholesterol efflux transporter, positively regulated by the PPAR γ -LXR α -ABCA1/ABCG1 signaling axis, and plays an important role in maintaining cholesterol homeostasis [25]. Modern pharmacological studies have shown that TCM exhibits multi-target, multi-pathway synergistic characteristics in the treatment of hyperlipidemia, which is distinct from the single-target action of statins. For example, berberine can simultaneously inhibit cholesterol synthesis and enhance RCT; paeoniflorin exerts dual regulation of cholesterol clearance and efflux by downregulating PCSK9 and upregulating LDLR and the LXRα-ABCG1 pathway [26]. In this study, we found that AMR-AR and FAMR-FAR interventions significantly restored hepatic LDL-C clearance capacity in high-fat diet-induced hyperlipidemic mice, improved circulating cholesterol uptake and utilization, and reestablished cholesterol efflux and RCT function. Notably, most previous TCM studies have focused on either the PCSK9-LDLR clearance axis or the PPARγ -LXRα-ABCG1 efflux axis as a single pathway, whereas our results suggest that AMR-AR and FAMR-FAR may coordinately regulate both pathways. This synergistic effect contributes to restoring cholesterol metabolic balance and provides mechanistic support for their therapeutic efficacy in improving hyperlipidemia.

Bile acid synthesis is the only irreversible pathway for cholesterol catabolism in the liver and is primarily controlled by CYP7A1 and CYP8B1, among which CYP7A1 is tightly regulated by the FXR-FGF15 feedback axis [27]. FXR and TGR5 alleviate hyperlipidemia by modulating lipid metabolism. In the distal ileum, bile acids activate FXR and induce FGF15 to enter the portal circulation, thereby suppressing hepatic bile acid synthesis [28]. Intestinal bile acid

reabsorption, mainly mediated by ASBT and OSTα/β, determines the efficiency of the enterohepatic circulation [29]. Furthermore, FXR activation induces the expression of ABCG5/ABCG8, promoting direct cholesterol efflux into the intestinal lumen [30]. Pharmacological studies on TCM have revealed that various TCM components exert lipid-lowering effects by regulating bile acid metabolism. For example, berberine activates the FXR-TGR5 pathway by modulating the gut microbiota and bile acid composition; Sanhuang Xiexin decoction regulates the expression of CYP7A1 and CYP27A1 via the FXR-FGF15 axis [31]. Our results show that a high-fat diet induces significant disruption of the bile acid metabolic profile in mice, which is partially restored following AMR-AR and FAMR-FAR intervention, with GCDCA exhibiting the most pronounced changes. Moreover, both treatments significantly upregulated the mRNA expression of FXR, FGF15, ASBT, and OSTα, sugrohepatic circulation transporters, our findings suggest that AMR-AR and FAMR-FAR coordinately regulate bile acid synthesis, enterohepatic circulation, and receptor-mediated signaling.

Serotonin (5-hydroxytryptamine, 5-HT), as an important gut-derived metabolic regulator, plays a pivotal role in the maintenance of energy homeostasis [32], lipid absorption, and the pathogenesis of metabolic disorders [33,34]. TPH1 is the rate-limiting enzyme for intestinal 5-HT synthesis [29], and its upregulation is considered a key molecular basis for diet-induced increases in peripheral 5-HT [35]. Previous studies have demonstrated that high-fat or high-carbohydrate diets markedly upregulate Tph1 expression in enterochromaffin (EC) cells, leading to elevated plasma 5-HT levels [36], which in turn promote the development of obesity, insulin resistance, and hepatic steatosis [37]. In the present study, TPH1 expression was significantly increased in hyperlipidemic mice, further supports a pathogenic role of gut-derived 5-HT in hyperlipidemia. Notably, pharmacological intervention markedly reduced TPH1 expression, suggesting that this treatment may attenuate peripheral 5-HT signaling at its source by suppressing intestinal 5-HT synthesis, thereby alleviating lipid metabolic disturbances. HTR4 is a major functional serotonin receptor in the intestine. Recent studies have identified HTR4 as a critical regulator of dietary fat absorption and chylomicron secretion. Peripheral 5-HT promotes apolipoprotein B48 – dependent chylomicron production through activation of HTR4, resulting in increased postprandial plasma triglyceride levels [38]. In this study, the expression of intestinal HTR4 was significantly upregulated in hyperlipidemic mice, suggesting that HTR4-mediated lipid transport is aberrantly activated under hyperlipidemic conditions. Following treatment, HTR4 expression was markedly downregulated, indicating that this intervention not only suppresses serotonin production but also attenuates downstream receptor-mediated signal amplification.

5 Conclusion

This study demonstrates that AMR-AR and FAMR-FAR exert pronounced lipid-lowering effects, as evidenced by significant reductions in serum TC, TG and LDL-C levels, accompanied by an increase in HDL-C levels in hyperlipidemic mice. Moreover, AMR-AR and FAMR-FAR treatments attenuated hepatic lipid accumulation and inflammatory infiltration, thereby ameliorating HFD-induced disturbances in lipid and bile acid metabolism. Notably, both interventions simultaneously downregulated the expression of TPH1 and HTR4 in the small intestine, effectively limiting 5-HT-driven lipid accumulation. Based on safe and effective medicinal-edible homologous herbal medicines, this study validates the feasibility of combined natural drug therapy for hyperlipidemia and provides new insights into its therapeutic management.

Abbreviation

ABCG1/5/8: ATP-binding cassette sub-family G member 1/5/8; AMR: atractylodis macrocephalae rhizoma; AR: atractylodis rhizoma; ASBT: apical sodium-dependent bile acid transporter; CYP7A1: cytochrome P450 family 7 subfamily A member 1; FAMR: fried atractylodis macrocephalae rhizoma with bran; FAR: fried atractylodis rhizoma with bran; FGF15: fibroblast growth factor 15; FXR: farnesoid X receptor; HTR4: 5-hydroxytryptamine receptor 4; LDLR: low-density lipoprotein receptor; LXRα: liver x receptor alpha; OST α : organic solute transporter alpha; PCSK9: proprotein convertase subtilisin/kexin type 9; PPAR γ : peroxisome proliferator-activated receptor gamma; SR-BI: scavenger receptor class B type I; TGR5: takeda G protein-coupled receptor 5; TPH1: tryptophan hydroxylase 1

Acknowledgements

We appreciate the great appreciate the great support from the Pharmaceutical Research Center, Academy of Chinese Medical Sciences, Zhejiang Chinese Medical University.

Conflicts of Interest

The authors declare that there is no conflict of interests.

Author Contributions

K.L.: Wrote the paper, Performed research, Analyzed data. F.D. and L.H.: Performed research, Contributed new methods or models. J.G. and Z.L. Conceived of or designed study. All authors read and approved the final manuscript.

Ethics Approval and Consent to Participate

All animal experimental protocols and procedures have been reviewed and approved by the Ethics Committee of the Experimental Animal Research Center of Zhejiang Chinese Medicine University, with ethics approval number of IACUC-20210726-07.

Funding

This research was supported by the Traditional Chinese Medicine Science and Technology Project of Zhejiang Province of China (Grant No. 2022ZA049; the Ningbo Public Welfare Program (2023S058), and Zhejiang Provincial Public Welfare Program (LGN22H280009, LTGN23H280003).

Availability of Data and Materials

The data presented in this study are available on request from the corresponding author.

Supplementary

Not applicable.

References

[1] Manolis AA, Manolis TA, Vouliotis A, et al. Metabolic dysfunction-associated steatotic liver disease and the cardiovascular system. *Trends in Cardiovascular Medicine* 2025; 35: 258-265.

[2] Hofbauer S, Wiesli P. Cme: Primäre und sekundäre hypercholesterinämie. *Praxis* 2020; 109: 755-762.

[3] Aguilar-Salinas CA, Gómez-Díaz RA, Corral P. New therapies for primary hyperlipidemia. *The Journal of Clinical Endocrinology & Metabolism* 2021; 107: 1216-1224.

[4] Girard J, Quadri H, Jiang B, et al. Fri091 treatment of secondary hyperlipidemia due to nephrotic syndrome. *Journal of the Endocrine Society* 2023; 7: bvad114.605.

[5] Wright AK, Kontopantelis E, Emsley R, et al. Cardiovascular risk and risk factor management in type 2 diabetes mellitus. *Circulation* 2019; 139: 2742-2753.

[6] Stewart J, McCallin T, Martinez J, et al. Hyperlipidemia. *Pediatrics In Review* 2020; 41: 393-402.

[7] Bikbov B, Purcell CA, Levey AS, et al. Global, regional, and national burden of chronic kidney disease, 1990–2017: A systematic analysis for the global burden of disease study 2017. *The Lancet* 2020; 395: 709–733.

[8] Zhang Y, Kishi H, Kobayashi S. Add-on therapy with traditional chinese medicine: An efficacious approach for lipid metabolism disorders. *Pharmacological Research* 2018; 134: 200-211.

[9] Xie Z, Li E, Gao G, et al. Zexie tang targeting fkbp38/mtor/srebps pathway improves hyperlipidemia. *Journal of Ethnopharmacology* 2022; 290: 115101.

[10] Yang SH, Zhu J, Wu WT, et al. Rhizoma atractylodis macrocephalae—assessing the influence of herbal processing methods and improved effects on functional dyspepsia. *Frontiers in Pharmacology* 2023; 14: 1-8.

[11] Song MY, Lim SK, Wang JH, et al. The root of atractylodes macrocephala koidzumi prevents obesity and glucose intolerance and increases energy metabolism in mice. *International Journal of Molecular Sciences* 2018; 19: 278.

[12] Heo G, Kim Y, Kim EL, et al. Atractylodin ameliorates colitis via pparα agonism. *International Journal of Molecular Sciences* 2023; 24: 802.

[13] Park YJ, Seo M, Cominguez DC, et al. Atractylodes chinensis water extract ameliorates obesity via promotion of the sirt1/ampk expression in high-fat diet-induced obese mice. *Nutrients* 2021; 13: 2992.

[14] Peng L, He M, Wang X, et al. Fast discrimination and quantification analysis of atractylodis rhizoma using nir spectroscopy coupled with chemometrics tools. *Journal of Agricultural and Food Chemistry* 2024; 72: 7707-7715.

[15] Liu Y, Yang X, Gan J, et al. Cb-dock2: Improved protein –ligand blind docking by integrating cavity detection, docking and homologous template fitting. *Nucleic Acids Research* 2022; 50: W159-W164.

[16] Shen J, Liu Q, Ning J, Li L. Elucidating the taste profile in black tea through molecular docking and molecular sensory science. *Food Chemistry* 2025; 145: 104.

[17] Li J, Lou Z, Huang J, et al. Exploring the effect of stir-fried atractylodis macrocephalae rhizoma and stir-fried atractylodis rhizoma on regulating water metabolism in the prevention and treatment of hyperlipidemia based on "spleen governing transportation and transformation of body fluids". *China Journal of Traditional Chinese Medicine and Pharmacy* 2024; 39: 168–172.

[18] Hoekstra M. Sr-bi as target in atherosclerosis and cardiovascular disease - A comprehensive appraisal of the cellular functions of sr-bi in physiology and disease. *Atherosclerosis* 2017; 258: 153-161.

[19] Steck TL, Lange Y. Is reverse cholesterol transport regulated by active cholesterol? *Journal of Lipid Research* 2023; 64: 385.

[20] Okumura M, Hamada A, Ohsaka F, et al. Expression of serotonin receptor htr4 in glucagon-like peptide-1-positive enteroendocrine cells of the murine intestine. *Pflügers Archiv - European Journal of Physiology* 2020; 472: 1521-1532.

[21] Akaki J, Tachi S, Nakamura N, et al. Promotive effect of bofutsushosan (fangfengtongshengsan) on lipid and cholesterol excretion in feces in mice treated with a high-fat diet. *Journal of Ethnopharmacology* 2018; 220: 1-8.

[22] Ripatti P, Rämö JT, Mars NJ, et al. Polygenic hyperlipidemias and coronary artery disease risk. *Circulation: Genomic and Precision Medicine* 2020; 13: e002725.

[23] Ouimet M, Barrett TJ, Fisher EA. Hdl and reverse cholesterol transport. *Circulation Research* 2019; 124: 1505-1518.

[24] Rizzolo D, Kong B, Taylor RE, et al. Bile acid homeostasis in female mice deficient in cyp7a1 and cyp27a1. *Acta Pharmaceutica Sinica B* 2021; 11: 3847-3856.

[25] Schoeler M, Caesar R. Dietary lipids, gut microbiota and lipid metabolism. *Reviews in Endocrine and Metabolic Disorders* 2019; 20: 461-472.

[26] Yang Y, Li X, Tang DL, et al. Paeoniflorin modulates trem-1/nf-κb/lxrα/abcg1 pathway to improve cholesterol metabolism and inflammation in hyperlipidemic rat. *International Journal of Molecular Sciences* 2026; 27: 3039.

[27] Russell DW. The enzymes, regulation, and genetics of bile acid synthesis. *Annual Review of Biochemistry* 2003; 72: 137-174.

[28] Massafra V, Pellicciari R, Gioiello A, van MSWC. Progress and challenges of selective farnesoid x receptor modulation. *Pharmacology & Therapeutics* 2018; 191: 162-177.

[29] Matthes S, Bader M. Peripheral serotonin synthesis as a new drug target. *Trends in Pharmacological Sciences* 2018; 39: 560-572.

[30] Lou Z, Han L, Qu Y, et al. Multi-omics identified thdca as a key contributor to hyperlipidemia and as a potential therapeutic agent. *Reviews in Cardiovascular Medicine* 2023; 24: 248.

[31] Xiao S, Zhang Z, Chen M, et al. Xiexin tang ameliorates dyslipidemia in high-fat diet-induced obese rats via elevating gut microbiota-derived short chain fatty acids production and adjusting energy metabolism. *Journal of Ethnopharmacology* 2019; 241: 112032.

[32] Hwang I, Nam JE, Choi W, et al. Serotonin regulates lipogenesis and endoplasmic reticulum stress in alcoholic liver disease. *Diabetes & Metabolism Journal* 2025; 49: 798-811.

[33] Blackett JW, Sun Y, Purpura L, et al. Decreased gut microbiome tryptophan metabolism and serotonergic

signaling in patients with persistent mental health and gastrointestinal symptoms after covid-19. *Clinical and Translational Gastroenterology* 2022; 13: 1-6.

[34] Nonogaki K. The regulatory role of the central and peripheral serotonin network on feeding signals in metabolic diseases. *International Journal of Molecular Sciences* 2022; 23: 1600.

[35] Koopman N, Katsavelis D, Ten Hove AS, et al. The multifaceted role of serotonin in intestinal homeostasis. *International Journal of Molecular Sciences* 2021; 22: 7987.

[36] Young RL, Lumsden AL, Martin AM, et al. Augmented capacity for peripheral serotonin release in human obesity. *International Journal of Obesity* 2018; 42: 1880-1889.

[37] Fu J, Ma S, Li X, et al. Long-term stress with hyperglucocorticoidemia-induced hepatic steatosis with vldl overproduction is dependent on both 5-ht2 receptor and 5-ht synthesis in liver. *International Journal of Biological Sciences* 2016; 12: 219-234.

[38] Raka F, Hoffman S, Nady A, et al. Peripheral serotonin controls dietary fat absorption and chylomicron secretion via 5-ht4 receptor in males. *Endocrinology* 2024; 165: bqae112.